G-CSF rescues the memory impairment of animal models of Alzheimer's disease

Kuen-Jer Tsai,[1] Yueh-Chiao Tsai,[2] and Che-Kun James Shen[1,2]

[1]Institute of Molecular Biology, Academia Sinica, Taipei 115, Taiwan, Republic of China
[2]Institute of Genome Sciences, National Yang-Ming University, Taipei 112, Taiwan, Republic of China

Most of the current clinical treatments for Alzheimer's disease (AD) are largely symptomatic and can have serious side effects. We have tested the feasibility of using the granulocyte colony-stimulating factor (G-CSF), which is known to mobilize hematopoietic stem cells (HSCs) from the bone marrow into the peripheral blood, as a therapeutic agent for AD. Subcutaneous administration of G-CSF into two different β-amyloid (Aβ)–induced AD mouse models substantially rescued their cognitive/memory functions. The rescue was accompanied by the accumulation of 5-bromo-2′deoxyuridine–positive HSCs, as well as local neurogenesis surrounding the Aβ aggregates. Furthermore, the level of acetylcholine in the brains of Tg2576 mice was considerably enhanced upon G-CSF treatment. We suggest that G-CSF, a drug already extensively used for treating chemotherapy-induced neutropenia, should be pursued as a novel, noninvasive therapeutic agent for the treatment of AD.

CORRESPONDENCE
Che-Kun James Shen:
ckshen@imb.sinica.edu.tw

The Journal of Experimental Medicine

Alzheimer's disease (AD) affects more than 12 million patients worldwide, and it accounts for most of the dementia diagnosed after the age of 60. The disease is clinically manifested by a global decline of cognitive function that progresses slowly. The characteristic features of AD brains are the formation of neurofibrillary tangles and the presence of senile plaques, the neurotoxicity of which are believed to be responsible for the neuronal loss and the degeneration of the cholinergic system in AD patients (1, 2). β-Amyloid (Aβ), which is the major extracellular component of the senile plaques, is generated from cleavage of the amyloid precursor protein, a transmembrane protein, to an amyloidogenic end product (3). The amount of Aβ needed to form the plaques correlates with the degree of neuronal damage and cognitive deficits (1, 2).

No treatments can stop AD today. Most of the current clinical treatments for AD are largely symptomatic, including the use of acetylcholinesterase inhibitors to improve cognitive ability and psychotropic drugs to modify patient behaviors (4). Treatments that focus on delaying the onset of symptoms and slowing the rate of disease progression are also being used. These strategies enhance the functions of the survival neuronal cells, and they include the uses of (a) tacrine, the first Food and Drug Administration–approved drug for AD therapy; (b) memantine, an *N*-methyl-D-aspartate antagonist; and (c) antioxidants such as vitamin E. Other likely promising therapies for AD include antiamyloid immunotherapy, amyloid vaccination, and the use of secretase inhibitors that prevent the formation of Aβ and neurofibrillary tangles (5). However, these therapies could all cause side effects and, consequently, clinical problems (4–6). AD is also one of the candidate diseases for the development of cell-regenerative strategies, because the transplantation of cells lacking the AD-causing mutation could replace the lost neurons and reconstitute the damaged neuronal connections.

G-CSF is a hematopoietic growth factor named for its role in the proliferation and differentiation of cells of the myeloic lineage. Administration of G-CSF mobilized hematopoietic stem cells (HSCs) from the bone marrow into the peripheral blood (7). The peripheral blood–derived HSCs have been used in place of bone marrow cells in transplantation for the regeneration of nonhematopoietic tissues such as skeletal muscle and the heart (8). G-CSF has been used extensively for >10 yr in the treatment of chemotherapy-induced neutropenia, as well as for bone marrow reconstitution and stem cell mobilization (9, 10). More recently, it has been shown that administration of G-CSF in stroke mouse models could induce neurogenesis near the damaged area of these mice, leading to neurological and functional recovery (11–13).

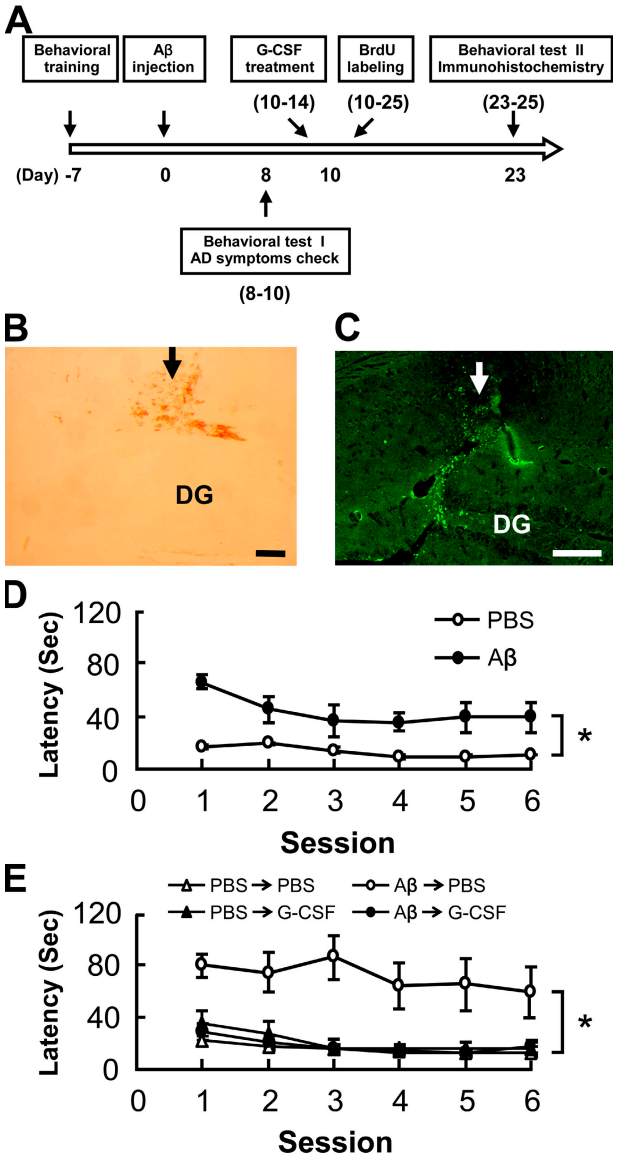

Figure 1. G-CSF treatment of an acutely induced mouse AD model. (A) Experimental design for the G-CSF treatment of an acutely induced mouse AD model. Starting from the first day (−7), the mice received behavioral training for six sessions in 3 d to learn the location of a submerged platform in the pool. The mice were then subjected to stereotaxic surgery for the injection of aggregated Aβ on day 0. 7 d after the Aβ injection, the water maze test (six sessions from days 8–10) was used to confirm the AD symptoms of the injected mice. Subsequently, the mice were injected subcutaneously with 50 μg/kg G-CSF once daily for 5 consecutive days (days 10–14). At the same time, they received daily intraperitoneal injections of 50 mg/kg BrdU for 16 consecutive days (days 10–25). The water maze test was next used to check the behavioral performance of mice (days 23–25). Finally, the mice were killed, and their brains were analyzed by immunohistochemistry. (B) Aβ staining (brown) of an AD mouse brain 7 d after the Aβ injection. The arrow points to the site of injection. (C) Thioflavin S staining of the Aβ deposits of another AD mouse brain 7 d after the Aβ injection. The arrow indicates the site of injection. Bars, 200 μm. (D) Mice injected with Aβ or PBS were subjected to the Morris water maze learning test 7 d after the injection. The learning/memory capabilities are expressed as the latencies exhibited in six consecutive sessions of the test ($n = 20$ for each group). (E) The latencies of AD and control mice with subcutaneous administration of G-CSF and PBS, respectively, as measured from the water maze learning task, are examined ($n = 10$ for each of the four groups). Data are means ± SEM. *, $P < 0.05$. DG, dentate gyrus.

In view of these properties of G-CSF and its potential applications in the treatment of diseases with neuronal damages, two different Aβ aggregate–induced AD mouse models were used to explore the possibility that G-CSF might be applied for therapy of AD. Interestingly, we found that G-CSF induced stem cell release from the bone marrow, stimulated neurogenesis surrounding the Aβ plaques in mouse brains, and substantially improved the neurological function of AD mice.

RESULTS AND DISCUSSION

G-CSF improved the neurological behavior of an acutely induced AD mouse model

Two different Aβ aggregate–induced AD mouse models were used to explore the possibility that G-CSF might be applied for therapy of AD. To set up an acutely induced AD model (14, 15), the protocol described in Fig. 1 A was followed. Mice were first trained in the Morris water maze task. 7 d later, aggregated Aβ was injected into the junction of the hippocampus and cortex of the mouse brains. Another 7 d were allowed for the injected mice to develop AD-like features (Fig. 1 A). As indicated by immunostaining with anti-Aβ (Fig. 1 B) and by staining with thioflavin S (Fig. 1 C), which identified the locations of the Aβ aggregates (14, 15), the Aβ aggregates indeed formed near the sites of injection in the mouse brains. At the same time, a behavior test using the Morris water maze task showed that mice receiving the Aβ injection were impaired in their learning/memory abilities (Fig. 1 D). To evaluate whether G-CSF could rescue the neurological defects of the Aβ-induced AD mice, the water maze task was again used to test the AD mice after injection with G-CSF or PBS, respectively, for 5 d (Fig. 1 A). As shown in Fig. 1 E, the latency of G-CSF–treated AD mice was significantly less than the PBS-treated AD mice. In fact, it was similar to those of the control mice injected with either G-CSF or PBS (Fig. 1 E). These data indicated that subcutaneous administration of G-CSF significantly restored the learning/memory function of mice with acutely induced AD features.

G-CSF stimulated stem cell mobilization and homing in the brains of AD mice

In previous experiments, it was found that G-CSF treatment stimulated the release of HSCs into blood circulation (7). Furthermore, proliferating cells accumulated near the damaged tissue regions, which likely contributed to the recovery from ischemic heart disease or stroke (8, 11). To examine whether similar events occurred in the acutely induced AD mice treated with G-CSF, we initially analyzed the blood cell counts of these mice in comparison to the controls.

Indeed, animals treated for 5 d with G-CSF exhibited a significant increase in their white blood cells (WBCs; Fig. 2 A) but not in their red blood cells or platelets (not depicted), suggesting that our G-CSF treatment of the mice also mobilized HSCs into their peripheral blood. We then used the cell-proliferation marker BrdU to follow the possible engraftment of G-CSF–mobilized HSCs in the brain (11, 12). As represented in Fig. 2 (B and C), a significant increase in $BrdU^+$ cells was observed in the brains of G-CSF–treated mice in contrast to those injected with PBS (Fig. 2 D). Furthermore, the $BrdU^+$ cells in the brains of AD mice treated with G-CSF are more concentrated near the Aβ aggregates, with decreased numbers radially distant from the sites of injection (Fig. 2 E).

Finally, it is known that administration of G-CSF mainly mobilizes $CD34^+$ HSCs from the bone marrow into the peripheral blood (16). To test whether the $BrdU^+$-proliferating cells observed in the brains of G-CSF–treated AD mice were derived from HSCs, double immunostaining with anti-BrdU and anti-CD34 was performed. As represented in Fig. 2 F, ~20% of the $BrdU^+$ cells in the cortex and hippocampus co-expressed CD34. The data in Fig. 2 indicated that injection of G-CSF into the acute, Aβ-induced AD mice mobilized the release of HSCs into the peripheral blood, and it significantly stimulated the increase of proliferating cells surrounding the Aβ aggregates that formed near the injection sites of Aβ.

G-CSF also improved the neurological behavior of a chronic AD mouse model, Tg2576

The second AD mouse model we used to test the therapeutic effect of G-CSF was Tg2576. Tg2576 mice overexpressed the human amyloid precursor protein with the Swedish mutation, and they developed AD-like features such as memory deficits and Aβ plaques in the brain (17, 18). The amyloid plaques began to accumulate in the brains of Tg2576 mice around the age of 9 mo, when the AD-like features started to develop (17). We initially checked the brains of 12-mo-old Tg2576 mice for the existence of Aβ aggregates and their learning/memory capabilities. Indeed, the Tg2576 mouse brains contained Aβ depositions throughout the cortex (Fig. 3 A) and hippocampus (Fig. 3 B). These Tg2576 mice also exhibited significantly impaired learning/memory in the water maze test (compare the latencies of WT→PBS with Tg2576→PBS from session 1; Fig. 3 C). The Tg2576 mice were then treated with PBS or G-CSF, respectively, for 5 d. As shown in Fig. 3 C, although the latencies were similar between the wild-type mice treated with G-CSF and PBS, respectively, throughout the test (sessions 1–6; Fig. 3 C), G-CSF treatment significantly reduced the latency of the Tg2576 mice when compared with the PBS-treated controls (Fig. 3 C). Similar to the experiments with the Aβ injection AD model, the G-CSF treatment also significantly increased the number of $BrdU^+$-proliferating cells in the damaged brains of Tg2576 mice (Fig. 3 D), which were spread throughout the cortex

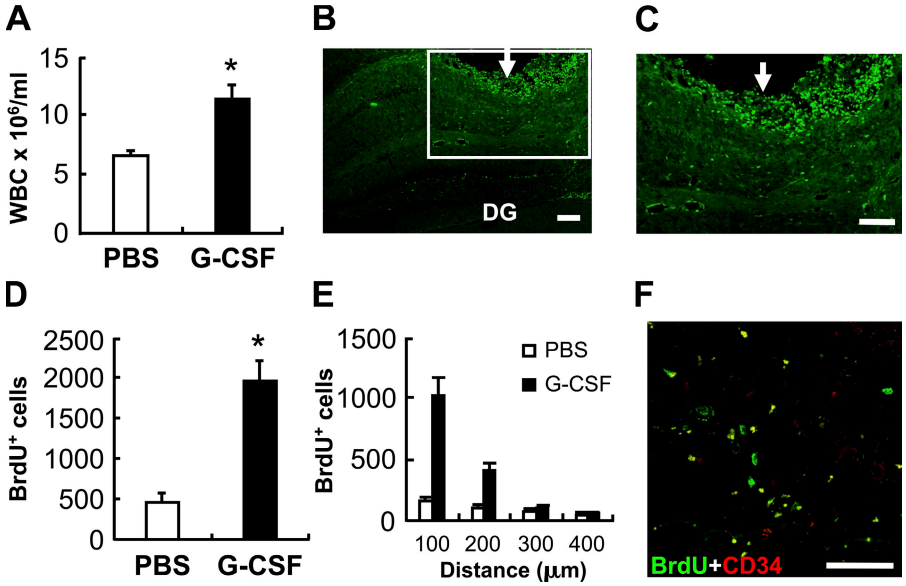

Figure 2. Stimulated increase of $BrdU^+$ cells by G-CSF. (A) WBC counts of AD mice administrated with PBS or G-CSF. The WBC counts were analyzed for mice after their treatment for 5 d with PBS or G-CSF ($n = 8$ for each group). (B and C) Immunostaining for $BrdU^+$ cells in a coronal brain section after BrdU incorporation of AD mice treated with G-CSF. The boxed area in B is magnified in C. The arrows indicate the injection site. Bar, 100 μm. (D) Comparison of the average numbers of $BrdU^+$ cells in the hemispheres of AD mice receiving BrdU and treated with PBS or G-CSF for 5 d ($n = 5$ for each group). The cell numbers were determined by immunostaining with anti-BrdU, as represented in B and C. (E) Distance dependence of the distribution of $BrdU^+$ cells. The numbers of $BrdU^+$ cells at different distances radially from the injection sites of the individual AD mice treated with G-CSF or PBS for 5 d and incorporated with BrdU were counted in the confocal microscope and averaged ($n = 5$ for each group). (F) Double immunostaining of BrdU and CD34. The brain sections from the AD mice with G-CSF treatment and BrdU incorporation were double stained with anti-BrdU (green) and anti-CD34 (red). Bar, 100 μm. Data in A, D, and E are means ± SEM. *, $P < 0.05$. DG, dentate gyrus.

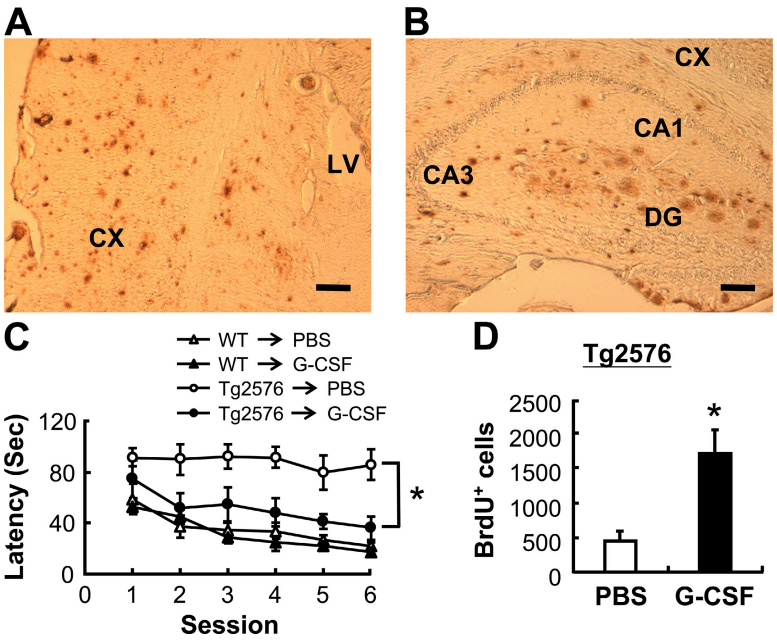

Figure 3. Rescue of the cognitive function of Tg2576 by G-CSF treatment. (A and B) Immunostaining of Aβ aggregates (brown) in the cortex (A) and hippocampus (B) of a 12-mo-old Tg2576 mouse. Bars, 200 μm. (C) The cognitive function of Tg2576 mice after subcutaneous administration of PBS or G-CSF was tested by the water maze learning task. The latencies from the tests of the wild-type control mice treated with PBS or G-CSF are included for comparison ($n = 9$ for the Tg2576→G-CSF group; $n = 7$ for the other three groups). The test data of one mouse unresponsive to the G-CSF treatment was not included in this figure. (D) Average numbers of $BrdU^+$ cells, as determined by anti-BrdU immunostaining, in the hemispheres of Tg2576 mice receiving BrdU and treated with PBS or G-CSF for 5 d ($n = 5$ for each group). Data are means ± SEM. *, $P < 0.05$. CA1, hippocampal CA1 layer; CA3, hippocampal CA3 layer; CX, cortex; DG, dentate gyrus; LV, lateral ventricle.

and hippocampus (not depicted). Thus, G-CSF also appeared to be an effective agent in rescuing the cognitive function of mice with a chronic pattern of AD development.

G-CSF–enhanced neurogenesis and the level of brain acetylcholine (ACh)

To examine the proportion of neuronal cells among the $BrdU^+$ cells in the brains of G-CSF–treated AD mice, double immunostaining was performed. For this, we used two additional antibodies directed against the microtubule-associated protein 2 (MAP2) and the vertebrate neuron-specific nuclear protein (NeuN), respectively. Both proteins are markers for most of the neuronal cell types throughout the mouse nervous system, including the cerebral cortex and the hippocampus (19). Single-section analysis of the immunostaining patterns of the acute AD mice, as represented in Fig. 4 (A–H), and Tg2576 mice (not depicted), as well as a three-dimensional reconstruction of multiple confocal images (not depicted), indicated that ∼40% of the $BrdU^+$ cells coexpressed NeuN (Fig. 4, I and J) or MAP2 (not depicted). These percentages are higher than those (∼20%) of the PBS-treated control mice (Fig. 4, I and J). These data suggested that G-CSF treatment caused an accumulation of proliferating, neuronal cells around the damaged brain areas of the AD mice. These cells very likely contributed to the rescue of the cognitive functions of both the acute, Aβ-induced AD mice and the Tg2576 mice by improving their neuronal plasticity.

To identify the molecular basis for the rescue of cognitive function by G-CSF, we analyzed the levels of ACh, as well as Aβ, in the brains of Tg2576 mice, with or without treatment by G-CSF. As shown in Fig. 5 A, G-CSF treatment increased the level of ACh by ∼20% when compared with the untreated Tg2576 mice and PBS-treated controls, respectively. In addition, we used both ELISA and immunohistochemistry to analyze the effect of G-CSF on the extent of brain amyloid aggregation. As shown in Fig. 5 B, there were no significant changes in the levels of both the SDS-soluble Aβ and the SDS-insoluble Aβ aggregates in the brains of Tg2576 mice treated with either PBS or G-CSF. Furthermore, the Aβ plaque burden in either the hippocampus or the cortex was similar among the G-CSF–treated, PBS-treated, and untreated Tg2576 mice (Fig. 5, C and D).

To examine whether the therapeutic effect of G-CSF could persist for a longer period of time, we analyzed the cognitive functions of Tg2576 mice 3 mo after the treatment. For this, 10 12-mo-old mice were divided into two groups and subjected to the water maze test before and 3 mo after subcutaneous administration with PBS and G-CSF, respectively (see Materials and methods). As shown in Fig. 5 E, the average latencies of the Tg2576 mice were similarly high with (Tg2576→PBS 3 mo) and without (Tg2576→PBS control) the PBS treatment. On the other hand, the G-CSF–treated mice remarkably showed a significantly better learning/memory capability even at 3 mo after the treatment (compare Tg2576→G-CSF 3 mo with

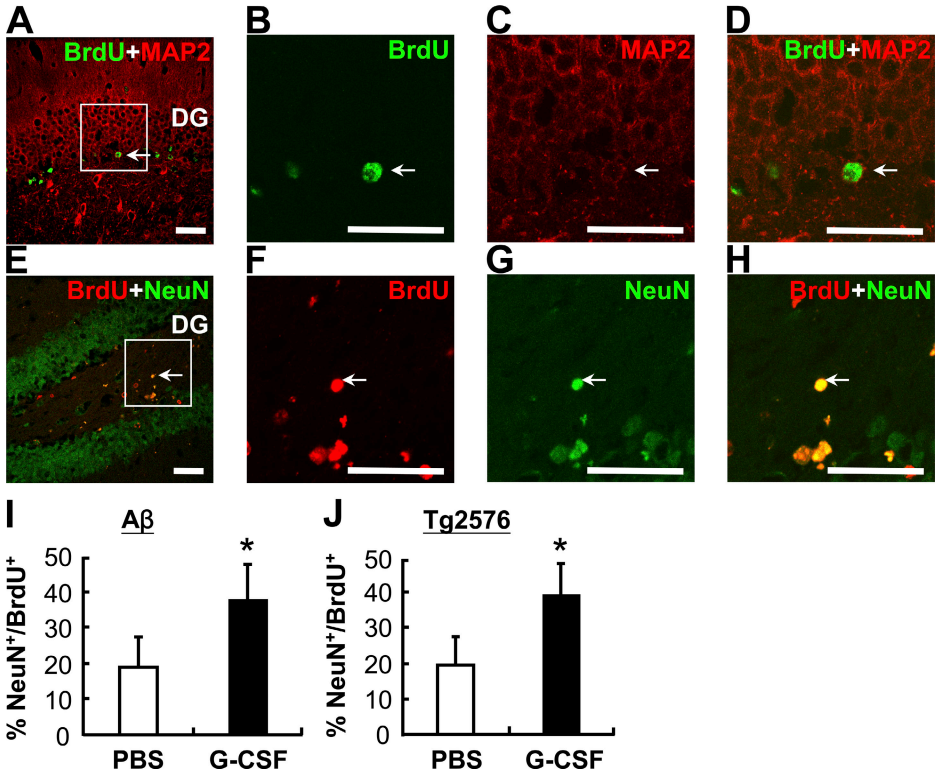

Figure 4. Enhancement of neurogenesis in AD mice by G-CSF. (A–H) Brain sections of the acute AD mice treated with G-CSF were double stained with anti-BrdU/anti-MAP2 (A–D) or with anti-BrdU/anti-NeuN (E–H). A and E provide low-magnification pictures of the staining patterns. The boxed areas in A and E are magnified in B–D and F–H, respectively. The arrows point to one example each of $BrdU^+/MAP2^+$ and $BrdU^+/NeuN^+$ cells. Bars, 50 μm. (I and J) Comparisons of the average percentages of $NeuN^+/BrdU^+$ cells in the hemispheres of Aβ-induced AD mice (I) or Tg2576 mice (J) treated with PBS or G-CSF for 5 d ($n = 5$ for each group). The cell numbers were determined by immunostaining, as represented in A–H. Data are means ± SEM. DG, dentate gyrus.

Tg2576→G-CSF control; Fig. 5 E). The data in Fig. 5 E indicated that administration of G-CSF could exert a long-lasting effect on the rescue of the cognitive functions of the Tg2576 AD mice.

One or a combination of the following could explain the cellular basis for rescue of the learning/memory deficiency in AD mice by G-CSF. First, similar to that proposed for the G-CSF effect on mice with ischemic heart disease or cerebral ischemia/stroke (8, 11), G-CSF could induce mobilization of bone marrow–derived HSCs that invaded the mouse brain areas damaged by the Aβ aggregates. As suggested by the significant increases of $BrdU^+/NeuN^+$ and $BrdU^+/MAP2^+$ cells near the Aβ aggregates in the brains of the acute AD mice or in the cortex/hippocampus of Tg2576 mice (Figs. 2 and 4), the HSCs differentiated into neuronal cells, thus leading to the functional and structural recovery of the brains of AD mice. Further, the fact that at least a portion (20%) of the $BrdU^+$ cells in the brains from an acute AD mouse model treated with G-CSF were also $CD34^+$, as exemplified in Fig. 2 F, provided the first direct evidence for G-CSF–induced mobilization of HSCs into the damaged brain regions. The different cytokines and trophic factors produced by HSCs within the cerebral tissue or within the microvasculature of an injured brain could also stimulate the proliferation, migration, and differentiation of neuronal progenitor cells (20–22), thus contributing to the functional and structural recoveries of the damaged brain.

Second, neuronal stem cells (NSCs) have been shown to reside in several regions in the adult brain, and they give rise to mature neuronal cells (23). Interestingly, G-CSF could induce the differentiation of NSCs in vitro, and this effect paralleled the in vivo finding that G-CSF also induced neurogenesis and subsequently enhanced functional recovery after cortical cerebral ischemia (12). Thus, G-CSF might also have enhanced the neurogenesis of NSCs near the Aβ aggregates and/or damaged brain regions of the AD mice. Finally, part of the rescuing effect of G-CSF on the AD mice might be caused by a direct protective role of G-CSF against programmed death of the neurons (24).

Notably, the treatment of patients with AD has been based largely on a strategy of enhancing the ACh-mediated transmission. Symptomatic benefits (cognitive, functional, and behavioral) have been observed in multiple clinical trials with agents known to inhibit acetylcholinesterase, which catalyses the breakdown of ACh. Our data in Fig. 5 A suggested that the rescue of the cognitive function of Tg2576 by G-CSF mice was partly caused by the increased level of ACh,

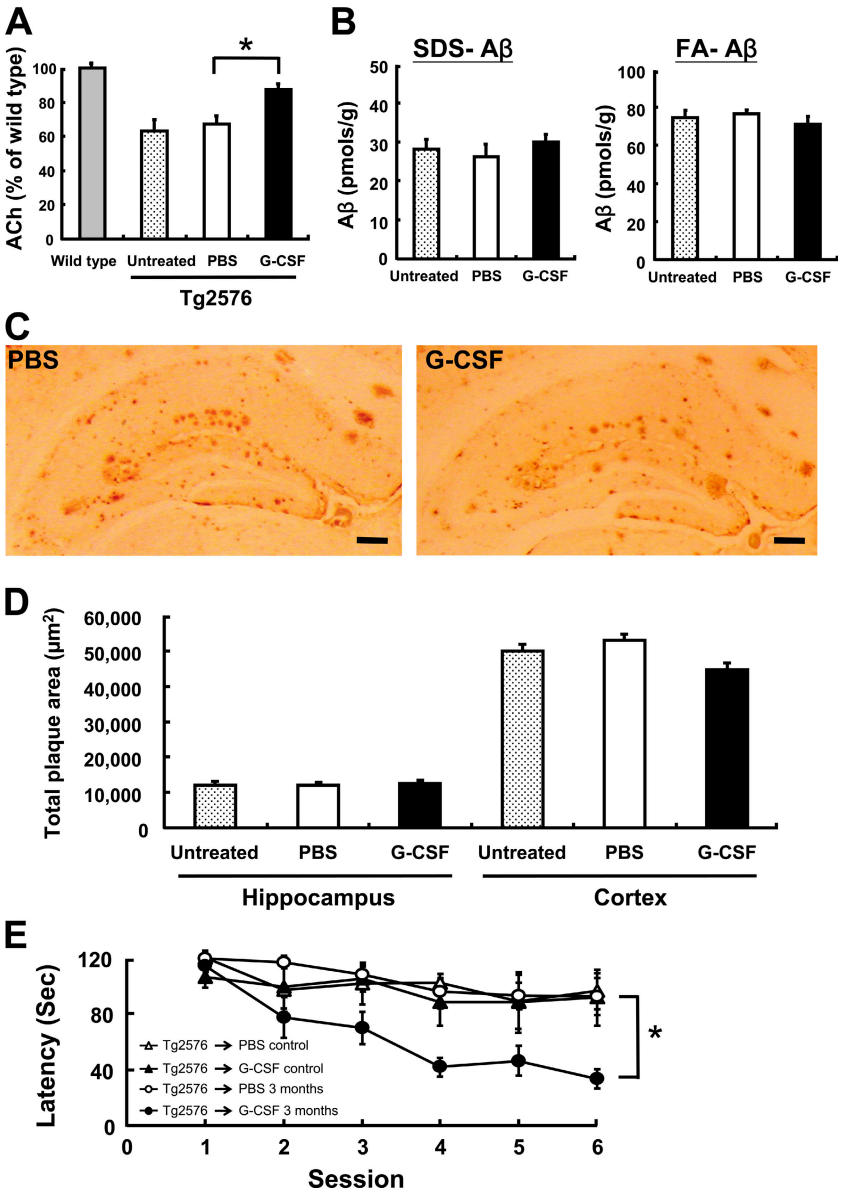

Figure 5. Effects of G-CSF treatment on the brain levels of ACh and Aβ. (A) Extents of ACh release in the brains of Tg2576 mice after subcutaneous administration with PBS or G-CSF. The extents are expressed as the percentages of the brain ACh level of the wild-type mice ($n = 5$ for each group). Note the relatively lower level of ACh in the brains of Tg2576 mice compared with the wild type, as well as the significant increase of the brain ACh amount of Tg2576 upon treatment with G-CSF but not with PBS. *, $P < 0.05$. (B) The levels of SDS-soluble Aβ (SDS-Aβ, left) and SDS-insoluble/formic acid–soluble Aβ (FA-Aβ, right) in the brains of untreated Tg2576 mice in comparison with Tg2576 mice after subcutaneous administration with PBS or G-CSF ($n = 5$ for each group). Note the insignificant differences among the three groups ($P > 0.1$ according to the Student's *t* test). (C and D) The Aβ plaque burden in the brains of untreated Tg2576 mice in comparison with Tg2576 mice after subcutaneous administration with PBS or G-CSF. The distribution patterns of the Aβ plaques in the hippocampus of PBS- and G-CSF–treated Tg2576 mice, respectively, are represented in C. Bars, 200 μm. The quantitative image analysis of the total areas of the Aβ plaque burden in the hippocampus or cortex of untreated, PBS-treated, and G-CSF–treated Tg2576 mice, respectively, is shown in D ($n = 3$ for each group). Note the insignificant differences among the three groups ($P > 0.1$ according to the Student's *t* test). (E) Long-lasting effect of G-CSF rescue of Tg2576 mice. The water maze test was applied to measure the cognitive functions of Tg2576 mice 3 mo after the subcutaneous administration of PBS or G-CSF. The latencies of the Tg2576 mice before the treatment with PBS or G-CSF (the controls) are included for comparison ($n = 5$ for each group). Data in A, B, D, and E are means ± SEM. *, $P < 0.05$.

likely as the result of a release of ACh from cholinergic neurons in the population of newly generated neuronal cells, as stimulated by G-CSF.

Our data have suggested the feasibility of using G-CSF as a novel therapeutic strategy for the treatment of AD. When compared with the drugs previously applied to Aβ-induced

AD animal models (e.g., ferulic acid [15] and cannabinoids [25]), the rescuing effect of G-CSF in the behavior test is at least equal. G-CSF is also as effective as other therapies such as the use of Aβ antibody (26). Notably, our data in Fig. 5 E showed that the rescuing effect of G-CSF may be long-lasting. We propose that G-CSF treatment of human AD patients would also mobilize autologous HSCs into circulation, enhance their translocation into the damaged brains, substantially repair the lesion areas, and, thus, rescue the memory dysfunction of the patients. The noninvasive nature of G-CSF treatment, when compared with the common practice of stem cell transplantation, makes it a potentially ideal AD drug for clinical trials. The combination of G-CSF with one or more of the other therapeutic ways would be another perspective direction for AD treatment.

MATERIALS AND METHODS

AD mouse models. Two different mouse models of AD were generated and/or bred for the test of G-CSF therapy. The acute Aβ-induced model was generated according to a previously described protocol (14, 15). 8-wk-old C57BL/6 male mice were purchased from the National Laboratorial Animal Center and bred at the Animal Facility of the Institute of Molecular Biology (IMB) at Academia Sinica. Experimental procedures for handling the mice followed the guidelines of the IMB. Animals were housed in a room maintained on a 12-h/12-h light/dark cycle (light on at 7:00 a.m.). The Aβ aggregate was prepared from a solution of 10 mM of soluble $A\beta_{(1-42)}$ (Sigma-Aldrich) in 0.01 M PBS, pH 7.4. The solution was incubated at 37°C for 3 d to form the aggregated Aβ and stored at −70°C. Animals were intraperitoneally anesthetized with 40 mg/kg sodium pentobarbital, and the injection of aggregated Aβ was made bilaterally into the dorsal hippocampus using a 26-gauge needle connected to a microsyringe (Hamilton). The animals were subjected to stereotaxic surgery with the incisor bar set at the following coordinates: 2 mm posterior to the bregma, 2.1 mm bilateral to the midline, and 1.8 mm ventral to the skull surface. The volume of injection was 1 μl of aggregated Aβ or 1 μl PBS, and 7 d were allowed for AD symptoms to develop in the subjects. For the chronic AD model, Tg2576 mice were purchased from Taconic and were bred as described in this section.

G-CSF treatment. For the acute AD model, 7 d after injection of the aggregated Aβ, mice were subcutaneously injected with 50 μg/kg of recombinant human G-CSF (Amgen Biologicals) once daily for 5 consecutive days (7, 11). The control animals were injected with PBS in parallel. More details are described in Fig. 1 A. Tg2576 mice were treated in a similar way.

Behavioral measurements. For spatial learning in the Morris water maze learning task, which was used as previously described (27), the animals were subjected to four trials per session and two sessions per day, with one session given in the morning and the other given in the afternoon. For a complete test, a total of six sessions over 3 d were given. In each of the four trials, the animals were placed at four different starting positions equally spaced around the perimeter of the pool in a random order. They were allowed 120 s to find the platform. If an animal could not find the platform in 120 s, it was guided to the platform. After mounting the platform, the animals were allowed to stay there for 20 s. The time that an individual mice took to reach the platform was recorded as the escape latency. For all the behavior tests in this study, the native mice received the spatial training for six sessions over 3 d to learn the location of a submerged platform in the pool. 7 d after the Aβ injection, the water maze test (six sessions over 3 d) was used to confirm the AD symptoms. The same water maze test was also used to check the behavioral performances of mice after G-CSF or PBS treatment. For Aβ-injected mice, the waiting period before the test was 14 d after the first injection (Fig. 1 E). For Tg2576 mice, the waiting period was either 14 d (Fig. 3 C) or 3 mo (Fig. 5 E).

BrdU labeling. BrdU (Sigma-Aldrich), a thymidine analogue that is incorporated into the DNA of dividing cells during S phase, was used for mitotic labeling. The labeling protocol followed those previously described (28). A cumulative labeling method was used to examine the population of proliferative cells, with the mice receiving daily intraperitoneal injections of 50 mg/kg BrdU for 16 consecutive days, starting on the first day of G-CSF injection. The $BrdU^+$ cells in both hemispheres of the hippocampus and cortex were digitally counted with the use of a 20× objective lens with a laser scanning confocal microscope (LSM510; Carl Zeiss MicroImaging, Inc.) via a computer imaging analysis system (Imaging Research). For each animal, 40 coronal sections (each 15-μm thick) throughout the hippocampus and cortex were analyzed. The image analysis was also used to examine the distributions of $BrdU^+$ cells radially surrounding the Aβ aggregates that formed near the microinjection sites.

Immunohistochemistry. Immunohistostaining was used to identify the locations of BrdU and different proteins in the mouse brain. Double immunofluorescence staining was performed to identify MAP2, NeuN, and CD34, respectively, in $BrdU^+$ cells. For this, the mouse monoclonal anti-BrdU (Chemicon) and Alex Fluor 488–conjugated goat anti–mouse antibodies (Invitrogen) were initially used, followed by treatment with the rabbit polyclonal anti-MAP2 (Chemicon) and Alex Fluor 555–conjugated donkey anti–rabbit antibodies (Invitrogen) for the identification of the neuronal dendrites. Alternatively, the anti-BrdU and Alex Fluor 555–conjugated donkey anti–mouse antibodies (Invitrogen) were used, followed by treatment with rabbit polyclonal Alex Fluor 488–conjugated anti-NeuN (Chemicon) antibodies to identify the neuronal nuclei. The rabbit polyclonal anti-CD34 (Serotec) and Alex Fluor 555–conjugated donkey anti–rabbit antibodies were used to identify HSCs. For thioflavin S staining (29), the brain sections were fixed to the slides with 4% formaldehyde in 0.1 M phosphate buffer and stained with 1% thioflavin S (Sigma-Aldrich) solution for 8 min. Sections were rapidly washed once in 100% ethanol and twice in 80% ethanol/water, rinsed for 10 min with water, and mounted with the mounting medium. All immunostaining sections were analyzed with a laser scanning confocal microscope. The green (Alex Fluor 488) and red (Alex Fluor 555) fluorochromes on the slides were excited by a laser beam at 488 and 543 nm, respectively.

ACh assay. For measuring ACh levels in the mouse brains, the mice were killed, and their brains were quickly removed and frozen on dry ice. The brains were homogenized on ice and immediately subjected to the ACh assay. The ACh levels in the brain extracts were then determined with the Amplex Red Acetylcholine/Acetylcholinesterase Assay Kit (Invitrogen), according to the manufacturer's instructions. The measurement was performed in a fluorescence microplate reader (PowerWave 340; BioTek) using excitation in the range of 530–560 nm and emission detection at 590 nm.

Quantifications of the Aβ levels and Aβ plaque burden. The levels of soluble and insoluble Aβ were quantified according to the procedures of Kawarabayashi et al. (30). The tissue samples were homogenized in 10 wet-weight volumes of PBS containing a cocktail of protease inhibitors (20 μg/ml each of pepstatin A, aprotinin, phosphoramidon, and leupeptin; 0.5 mM PMSF; and 1 mM EGTA). The samples were briefly sonicated (10 W, 2 × 5 s) and centrifuged at 100,000 *g* for 20 min at 4°C. The soluble fraction (supernatant) was used for the Aβ ELISA assay. To quantitate the insoluble Aβ/Aβ aggregates, the SDS-insoluble pellet was sonicated and dissolved in 70% formic acid. The extract was neutralized with 0.25 M Tris, pH 8, containing 30% acetonitrile and 5 M NaOH before loading onto an ELISA plate. The protein-containing samples were subjected to assay by the Aβ ELISA kit (Sigma-Aldrich), and the signals at 450 nm were detected using a multiwell plate reader.

To quantify the Aβ plaque burden in the mouse brains, the method of Janus et al. (26) was followed. Eight sections from each cerebral hemisphere were immunostained with anti-Aβ antibody (Chemicon) and visualized with diaminobenzidine. The plaque burden was analyzed using ImageJ

software (National Institutes of Health), the brain area (hippocampus or cortex) was outlined, and the area and number of plaques in the outlined structure were recorded.

Statistical analysis. Data are reported as means ± SEM. Independent experiments were compared using the Student's *t* test. Differences, indicated by asterisks, were considered statistically significant at $P < 0.05$.

We thank Dr. Hung Li for many stimulating and helpful discussions.

This study was supported by Academia Sinica. K.-J. Tsai is an Academia Sinica Postdoctoral Fellow, and C.-K. J. Shen is an Academia Sinica Investigator Awardee.

The authors have no conflicting financial interests.

Submitted: 27 November 2006
Accepted: 20 April 2007

REFERENCES

1. Mattson, M.P. 2004. Pathways towards and away from Alzheimer's disease. *Nature*. 430:631–639.
2. Blennow, K., M.J. de Leon, and H. Zetterberg. 2006. Alzheimer's disease. *Lancet*. 368:387–403.
3. Kang, J., H.G. Lemaire, A. Unterbeck, J.M. Salbaum, C.L. Masters, K.H. Grzeschik, G. Multhaup, K. Beyreuther, and B. Muller-Hill. 1987. The precursor of Alzheimer's disease amyloid A4 protein resembles a cell-surface receptor. *Nature*. 325:733–736.
4. Francis, P.T., A. Nordberg, and S.E. Arnold. 2005. A preclinical view of cholinesterase inhibitors in neuroprotection: do they provide more than symptomatic benefits in Alzheimer's disease? *Trends Pharmacol. Sci*. 26:104–111.
5. Schenk, D. 2002. Amyloid-beta immunotherapy for Alzheimer's disease: the end of the beginning. *Nat. Rev. Neurosci*. 3:824–828.
6. Citron, M. 2004. Strategies for disease modification in Alzheimer's disease. *Nat. Rev. Neurosci*. 5:677–685.
7. Bodine, D.M., N.E. Seidel, M.S. Gale, A.W. Nienhuis, and D. Orlic. 1994. Efficient retrovirus transduction of mouse pluripotent hematopoietic stem cells mobilized into the peripheral blood by treatment with granulocyte colony-stimulating factor and stem cell factor. *Blood*. 84:1482–1491.
8. Orlic, D., J. Kajstura, S. Chimenti, F. Limana, I. Jakoniuk, F. Quaini, B. Nadal-Ginard, D.M. Bodine, A. Leri, and P. Anversa. 2001. Mobilized bone marrow cells repair the infarcted heart, improving function and survival. *Proc. Natl. Acad. Sci. USA*. 98:10344–10349.
9. Sheridan, W.P., G. Morstyn, M. Wolf, A. Dodds, J. Lusk, D. Maher, J.E. Layton, M.D. Green, L. Souza, and R.M. Fox. 1989. Granulocyte colony-stimulating factor and neutrophil recovery after high-dose chemotherapy and autologous bone marrow transplantation. *Lancet*. 2:891–895.
10. Weaver, C.H., C.D. Buckner, K. Longin, F.R. Appelbaum, S. Rowley, K. Lilleby, J. Miser, R. Storb, J.A. Hansen, and W. Bensinger. 1993. Syngeneic transplantation with peripheral blood mononuclear cells collected after the administration of recombinant human granulocyte colony-stimulating factor. *Blood*. 82:1981–1984.
11. Shyu, W.C., S.Z. Lin, H.I. Yang, Y.S. Tzeng, C.Y. Pang, P.S. Yen, and H. Li. 2004. Functional recovery of stroke rats induced by granulocyte colony-stimulating factor-stimulated stem cells. *Circulation*. 110:1847–1854.
12. Schneider, A., C. Kruger, T. Steigleder, D. Weber, C. Pitzer, R. Laage, J. Aronowski, M.H. Maurer, N. Gassler, W. Mier, et al. 2005. The hematopoietic factor G-CSF is a neuronal ligand that counteracts programmed cell death and drives neurogenesis. *J. Clin. Invest*. 115:2083–2098.
13. Kawada, H., S. Takizawa, T. Takanashi, Y. Morita, J. Fujita, K. Fukuda, S. Takagi, H. Okano, K. Ando, and T. Hotta. 2006. Administration of hematopoietic cytokines in the subacute phase after cerebral infarction is effective for functional recovery facilitating proliferation of intrinsic neural stem/progenitor cells and transition of bone marrow-derived neuronal cells. *Circulation*. 113:701–710.
14. Stephan, A., S. Laroche, and S. Davis. 2001. Generation of aggregated beta-amyloid in the rat hippocampus impairs synaptic transmission and plasticity and causes memory deficits. *J. Neurosci*. 21:5703–5714.
15. Yan, J.J., J.Y. Cho, H.S. Kim, K.L. Kim, J.S. Jung, S.O. Huh, H.W. Suh, Y.H. Kim, and D.K. Song. 2001. Protection against beta-amyloid peptide toxicity in vivo with long-term administration of ferulic acid. Protection against beta-amyloid peptide toxicity in vivo with long-term administration of ferulic acid. *Br. J. Pharmacol*. 133:89–96.
16. Grigg, A.P., A.W. Roberts, H. Raunow, S. Houghton, J.E. Layton, A.W. Boyd, K.M. McGrath, and D. Maher. 1995. Optimizing dose and scheduling of filgrastim (granulocyte colony-stimulating factor) for mobilization and collection of peripheral blood progenitor cells in normal volunteers. *Blood*. 86:4437–4445.
17. Hsiao, K., P. Chapman, S. Nilsen, C. Eckman, Y. Harigaya, S. Younkin, F. Yang, and G. Cole. 1996. Correlative memory deficits, Abeta elevation, and amyloid plaques in transgenic mice. *Science*. 274:99–102.
18. Ashe, K.H. 2001. Learning and memory in transgenic mice modeling Alzheimer's disease. *Learn. Mem*. 8:301–308.
19. Brazelton, T.R., F.M.V. Rossi, G.I. Keshet, and H.M. Blau. 2000. From marrow to brain: expression of neuronal phenotypes in adult mice. *Science*. 290:1775–1779.
20. Chopp, M., and Y. Li. 2002. Treatment of neural injury with marrow stromal cells. *Lancet Neurol*. 1:92–100.
21. Majka, M., A. Janowska-Wieczorek, J. Ratajczak, K. Ehrenman, Z. Pietrzkowski, M.A. Kowalska, A.M. Gewirtz, S.G. Emerson, and M.Z. Ratajczak. 2001. Numerous growth factors, cytokines, and chemokines are secreted by human CD34(+) cells, myeloblasts, erythroblasts, and megakaryoblasts and regulate normal hematopoiesis in an autocrine/paracrine manner. *Blood*. 97:3075–3085.
22. Williams, L.R., S. Varon, G.M. Peterson, K. Wictorin, W. Fischer, A. Bjorklund, and F.H. Gage. 1986. Continuous infusion of nerve growth factor prevents basal forebrain neuronal death after fimbria fornix transection. *Proc. Natl. Acad. Sci. USA*. 83:9231–9235.
23. Ming, G.L., and H. Song. 2005. Adult neurogenesis in the mammalian central nervous system. *Annu. Rev. Neurosci*. 28:223–250.
24. Schabitz, W.R., R. Kollmar, M. Schwaninger, E. Juettler, J. Bardutzky, M.N. Scholzke, C. Sommer, and S. Schwab. 2003. Neuroprotective effect of granulocyte colony-stimulating factor after focal cerebral ischemia. *Stroke*. 34:745–751.
25. Ramirez, B.G., C. Blazquez, T. Gomez del Pulgar, M. Guzman, and M.L. de Ceballos. 2005. Prevention of Alzheimer's disease pathology by cannabinoids: neuroprotection mediated by blockade of microglial activation. *J. Neurosci*. 25:1904–1913.
26. Janus, C., J. Pearson, J. McLaurin, P.M. Mathews, Y. Jiang, S.D. Schmidt, M.A. Chishti, P. Horne, D. Heslin, J. French, et al. 2000. A beta peptide immunization reduces behavioural impairment and plaques in a model of Alzheimer's disease. *Nature*. 408:979–982.
27. Tsai, K.J., S.K. Chen, Y.L. Ma, W.L. Hsu, and E.H. Lee. 2002. sgk, a primary glucocorticoid-induced gene, facilitates memory consolidation of spatial learning in rats. *Proc. Natl. Acad. Sci. USA*. 99:3990–3995.
28. Zhang, R.L., Z.G. Zhang, L. Zhang, and M. Chopp. 2001. Proliferation and differentiation of progenitor cells in the cortex and the subventricular zone in the adult rat after focal cerebral ischemia. *Neuroscience*. 105: 33–41.
29. Wyss-Coray, T., C. Lin, F. Yan, G.Q. Yu, M. Rohde, L. McConlogue, E. Masliah, and L. Mucke. 2001. TGF-beta1 promotes microglial amyloid-beta clearance and reduces plaque burden in transgenic mice. *Nat. Med*. 7:612–618.
30. Kawarabayashi, T., L.H. Younkin, T.C. Saido, M. Shoji, K.H. Ashe, and S.G. Younkin. 2001. Age-dependent changes in brain, CSF, and plasma amyloid β protein in the Tg2576 transgenic mouse model of Alzheimer's disease. *J. Neurosci*. 21:372–381.